

Miktoarm Star Micelles Containing Curcumin Reduce Cell Viability of Sensitized Glioblastoma

Ghareb M Soliman^{1-3#}, Anjali Sharma², Yiming Cui¹, Rishi Sharma², Ashok Kakkar^{2**} and Dusica Maysinger^{1**}

¹Department of Pharmacology and Therapeutics, McGill University, Canada

²Department of Chemistry, McGill University, Canada

³Department of Pharmaceutics, Faculty of Pharmacy, Assiut University, Egypt

#Author contributed equally

Abstract

Glioblastoma multiforme (GBM) is the most common and lethal primary intracranial tumor in humans. Monotherapeutic interventions have not been successful. The objective of the current studies was to establish the effective combination therapy consisting of pifitrin as a sensitizer, and curcumin as therapeutic incorporated into miktoarm micelles. A₂B type miktoarm stars were prepared using a combination of click chemistry with ring opening polymerization on a core with orthogonal functionalities. These self-assemble into spherical micelles with hydrophobic core and hydrophilic corona structure. Micellar delivery systems for curcumin based on these miktoarm star polymers were prepared, characterized and tested on cultures sensitized with pifitrin. The results show that: (1) pifitrin and temozolamide in combination with curcumin cause significant cell death compared with the individual therapeutics (incorporated or not in micelles), and (2) repeated exposure to the same treatments is necessary to fully prevent a re-growth of glioblastoma cells both in 2D and 3D cultures. Although the incorporation of curcumin into A₂B star polymer micelles did not increase the extent of cell death compared with curcumin alone, the advantage of micelles is that they significantly increase the aqueous solubility of curcumin and sustain its release; this will likely reduce the frequency of its administration required to be effective *in vivo*. A₂B miktoarm polymers could be a new viable delivery system for curcumin and other anticancer drugs with similar limitations.

Keywords: Curcumin; Self-assembly systems; Miktoarm star micelles; Glioblastoma multiforme; Cell death; Pifitrin; Spheroids

Introduction

Glioblastoma multiforme (GBM) is the most common and lethal intracranial tumor in humans due to its uncontrolled cellular proliferation, diffuse infiltration, propensity for necrosis, robust angiogenesis, intense resistance to apoptosis, rampant genomic instability, significant intra-tumoral heterogeneity (cytopathology, transcriptional, genomic), and a putative cancer stem cell component [1,2].

The major causes of primary glioblastomas are not well known, but often involve gene multiplications, deletions and mutations affecting growth factor receptor signaling. The response rate to treatment with temozolamide alone in patients with malignant gliomas is 5.4% [3]. Temozolamide and bevacizumab (anti-angiogenic, humanized monoclonal antibody vs. VEGF-A) are often used in combination with other treatments such as IFN α , irinotecan (topoisomerase-I inhibitor), doxorubicin, and alkylating agents such as carmustine and lomustine (nitrosoureas). Gliadel (carmustine wafers made of biodegradable polifeprosan 20 polymer) have shown an increase in median survival by 8 weeks in patients with recurrent glioblastoma [4]. Micellar nano-delivery systems for several drugs for the treatment of GBM have been developed and reviewed [5]. For instance, a micellar system based on amphiphilic peptides and incorporating bis-chloroethylnitrosourea (BCNU) and vascular endothelial growth factor (VEGF) small interfering RNA (VEGF-siRNA), was prepared and tested in C6 glioblastoma cells [6]. The micelles showed better delivery of BCNU into the cells and remarkably reduced expression of VEGF. In another recent study, polymeric micelles coated with cyclic Arg-Gly-Asp (cRGD) ligand molecules showed highly efficient anticancer drug delivery to U87MG tumors [7].

Curcuminoids are active components in perennial plant Curcuma longa. Curcuminoids have been used for millennia as folk medicines

in turmeric powder. More recent studies with isolated or purified extracts or individual curcuminoids suggested this class of compounds as putative therapeutics for various diseases, including diabetes, neurodegenerative disorders, cardiovascular disease and arthritis [8-10]. Curcumin is a pleiotropic agent modulating several signal survival transduction pathways and an attempt to block these pathways simultaneously is a current way of approaching the multidrug therapy of GBM [11]. Curcumin has low bioavailability, poor aqueous solubility and poor stability [12,13]. In aqueous media, curcumin undergoes rapid hydrolytic degradation, which is pH-dependent and occurs faster at neutral-basic conditions [14]. Further, curcumin has rapid metabolism, and rapid systemic elimination [12]. In order to overcome these hurdles, curcumin has been incorporated into several drug delivery systems [9]. Among those, polymeric micelles based on miktoarm star polymers have received a considerable attention. Miktoarm stars can be synthetically articulated using click chemistry for enhancing drug incorporation into their micelles [15-20]. Amphiphilic miktoarm star polymers spontaneously form nanoscale core/shell

***Corresponding author:** Ashok Kakkar, Department of Chemistry, McGill University, Canada, Tel: +1-514-398-6912; Fax: +1-514-398-3797; E-mail: ashok.kakkar@mcgill.ca

Dusica Maysinger, Department of Pharmacology and Therapeutics, McGill University, Canada, Tel: +1-514-398-1264; Fax: +1-514-398-6690; E-mail: dusica.maysinger@mcgill.ca

Received March 07, 2014; Accepted April 07, 2014; Published April 09, 2014

Citation: Soliman GM, Sharma A, Cui Y, Sharma R, Kakkar A, et al. (2014) Miktoarm Star Micelles Containing Curcumin Reduce Cell Viability of Sensitized Glioblastoma. J Nanomedicine Biotherapeutic Discov 4: 124. doi:10.4172/2155-983X.1000124

Copyright: © 2014 Soliman GM, et al. This is an open-access article distributed under the terms of the Creative Commons Attribution License, which permits unrestricted use, distribution, and reproduction in any medium, provided the original author and source are credited.

structures in aqueous environments, where hydrophobic polymer arms form the core of the micelles and hydrophilic ones form corona [21,22]. The core of these micelles can be used to load hydrophobic drugs in order to overcome their insolubility in water, control their release and protect them from rapid degradation and metabolism in the body. In addition to this, the hydrophilic corona enhances their blood circulation time and helps them deliver the drug to its target [23,24]. Thus, we investigated the utility of A₂B star polymers as nanocarriers for curcumin.

The overall objective of this study was to show that curcumin incorporated into A₂B micelles or combined with several other agents inhibit survival/proliferation of GBM cells grown in 2D monolayer and 3D spheroid cultures. A library of A₂B mikroarm polymers was synthesized and characterized using several techniques. The micellization behavior in aqueous solution was also studied together with the kinetics of curcumin release. Mikroarm micelles with or without curcumin were tested to establish concentration-dependent cell growth inhibition, cell death and spheroid disintegration. The experiments also included pifitrin and temozolamide in combination with curcumin to promote tumor cell elimination. Results suggest that only drug combination and multiple exposures of GBM cells to these treatments significantly reduce tumor cell viability and prevent their re-growth in 2D and 3D cultures.

Materials and Methods

Reagents and materials

Water was deionized using a Millipore Milli-Q system. Curcumin, temozolamide, ϵ -caprolactone (99%), tin (II) 2-ethylhexanoate (95%), 3-(4,5-dimethylthiazol-2-yl)-2,5-diphenyl tetrazolium bromide (MTT), copper(II) sulfate pentahydrate (CuSO₄•5H₂O) (>98.0%), sodium ascorbate (NaAsc, crystalline, 98%), Bisbenzimidazole H 33258 (Hoechst stain) (861405), and trypsin/EDTA (0.25%) were purchased from Sigma Aldrich, St. Louis, MO, and used as received. All reactions were performed under dry conditions in an inert environment using distilled solvents. Flash chromatography was performed using 60 Å (230-400 mesh) silica gel from EMD Chemicals Inc. Dialysis membranes (Spectra/por, MWCO: 6-8 kDa, unless otherwise indicated) were purchased from Fisher Scientific (Rancho Dominguez, CA). Penicillin, streptomycin, Griess reagent (1% sulphanilamide, 0.1% N-(1-naphthyl)-ethylenediaminedihydrochloride, and 5% phosphoric acid), and fetal bovine serum were purchased from Invitrogen (Carlsbad, CA). ϵ -Caprolactone was dried over calcium hydride for 24 h and distilled under reduced pressure prior to use. 2-(2-Imino-4,5,6,7-tetrahydrobenzothiazol-3-yl)-1-p-tolyethanone (pifithrin- α) (506132) was from Calbiochem (Darmstadt, Germany). Flat bottom 24-well and 96-well tissue culture plates were from SARSTEDT (Newton, NC).

Synthesis and characterization of A₂B mikroarm polymers

Compounds 1 and 2 (Figure 1) were synthesized using an adaptation of our previously published procedures [18]. PEG₇₅₀-azide was synthesized using a reported method [25]. The synthesis of polymers (3a-f) was carried out using a general synthetic procedure as outlined below for 3a, and by keeping polyethylene glycol (PEG) molecular weight constant, and varying polycaprolactone (PCL) molecular weight.

Compound 3a (PEG₇₅₀)₂-PCL₄₇₀₀: A solution of compound 2 ((PEG₇₅₀)₂-OH, 100 mg, 0.056 mmoles) in dry toluene (2 ml) was placed in a flame-dried two neck round bottom flask fitted with a condenser. The solution was degassed by evacuation, and distilled

ϵ -caprolactone (0.28 mL, 2.548 mmoles) was added under nitrogen with a syringe through the rubber septum. A nitrogen purged solution of Sn(II) 2-ethylhexanoate (2 mg, 0.005 mmoles) in toluene (1 mL) was then added to the reaction flask, and the mixture was refluxed for 24 h. The reaction mixture was then cooled to room temperature, and the solvent was removed under vacuum. The product was dissolved in dichloromethane and precipitated using cold methanol. The polymer was filtered and washed with diethyl ether to yield a white powder. ¹H NMR (500 MHz, CDCl₃): δ (ppm) 1.30-1.41 (m, -CH₂PCL), 1.55-1.65 (m, -CH₂PCL), 2.27-2.36 (m, -CH₂PCL), 3.35 (s, 6H, -OCH₃), 3.51-3.65 (m, PEG H), 3.87 (t, 4H, -CH₂OCH₃), 4.04 (t, -CH₂PCL), 4.54 (t, -CH₂CH₂ triazole), 5.01 (s, 2H, -OCH₃), 5.14 (s, 4H, -OCH₂ triazole), 6.58 (m, 3H, ArH), 7.82 (s, 2H, triazole H). ¹³C {¹H} NMR (CDCl₃) δ ppm 24.5, 25.5, 28.3, 32.3, 34.0, 50.3, 59.0, 62.0, 62.5, 64.1, 65.8, 69.4, 70.5, 71.9, 101.4, 107.1, 110.0, 124.1, 143.5, 159.5, and 173.5 GPC: Mn=6540, polydispersity index (PDI)=1.57.

Mikroarm stars (3b-f) were synthesized using a similar procedure as described above for 3a.

Compound 3b (PEG₇₅₀)₂-PCL₇₈₀₀: Compound 2 (100 mg, 0.06 mmoles) and ϵ -caprolactone (0.5 mL, 4.530 mmoles) GPC: Mn=9632, PDI=1.28.

Compound 3c (PEG₇₅₀)₂-PCL₈₈₀₀: Compound 2 (100 mg, 0.06 mmoles) and ϵ -caprolactone (0.56 mL, 5.096 mmoles) GPC: Mn=10,605, PDI=1.38.

Compound 3d (PEG₇₅₀)₂-PCL_{10,300}: Compound 2 (50 mg, 0.028 mmoles) and ϵ -caprolactone (0.31 mL, 2.831 mmoles) GPC: Mn=12,105, PDI=1.49.

Compound 3e (PEG750)2-PCL12,600: Compound 2 (50 mg, 0.028 mmoles) and ϵ -caprolactone (0.37 mL, 3.39 mmoles) GPC: Mn=14,327, PDI=1.21.

Compound 3f (PEG₇₅₀)₂-PCL_{14,200}: Compound 2 (50mg, 0.028mmoles) and ϵ -caprolactone (0.43 mL, 3.96 mmoles) GPC: Mn=16,000, PDI=1.27.

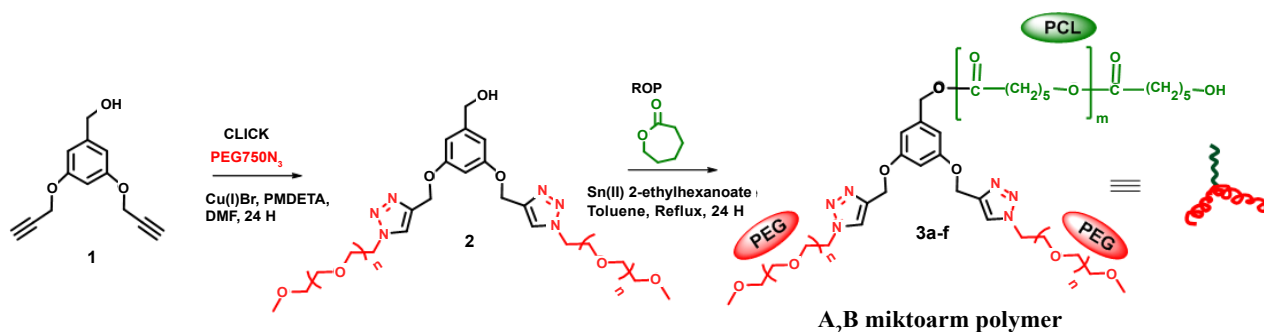
Preparation of mikroarm micelles

Mikroarm micelles were prepared by the co-solvent evaporation method [22]. Specific weights of the polymer and drug (drug/polymer ratio of 0-50 wt. %) were dissolved in 1.5 mL of acetone. The solution was added dropwise (1 drop/10 s) to 3 mL of magnetically stirred deionized water. The mixture was stirred in the dark for 24 h to remove acetone and trigger micelle formation. The mixture was filtered through a 0.45 μ m PVDF filter to remove the free (untrapped) drug. Aliquots of the micellar solutions were tested by dynamic light scattering (DLS) to determine the hydrodynamic diameter (DH) and polydispersity index (PDI) of the micelles. Aliquots of the solution were diluted 10 times by acetonitrile and used to determine drug content of the micelles by an HPLC assay.

Characterization

NMR spectra were recorded on a 500 MHz Varian spectrometer at ambient temperature. The chemical shifts in ppm are reported relative to tetramethylsilane as an internal standard for ¹H and ¹³C {¹H} NMR spectra. Molecular weight and polydispersity index (PDI) were characterized by GPC (Waters Breeze) using THF as the mobile phase. The GPC was equipped with three Waters Styragel HR columns (molecular weight measurement ranges: HR1: 10²-5 \times 10³ g mol⁻¹, HR2: 5 \times 10²-2 \times 10⁴ g mol⁻¹, HR3: 5 \times 10³-6 \times 10⁵ g mol⁻¹) and a guard column.

A) Synthesis of A₂B mikroarm star polymers



B) Self assembly and drug loading

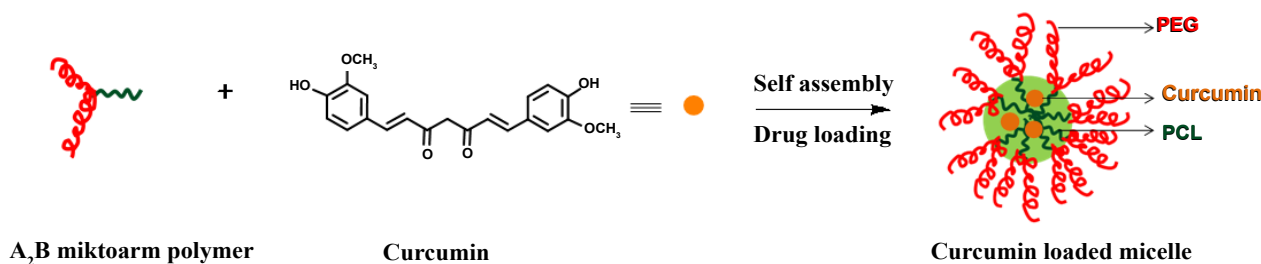


Figure 1: (A) Synthesis of A₂B mikroarm polymers: A (Hydrophilic polyethylene glycol, PEG) and B (Hydrophobic polycaprolactone, PCL). (B) Schematic illustration of micelle formation and curcumin loading.

The columns were operated at 40°C and a mobile phase flow rate of 0.3 ml min⁻¹ during analysis. The GPC was also equipped with both ultraviolet (UV 2487) and differential refractive index (RI 2410) detectors. The molecular weight measurements were calibrated relative to poly (styrene) narrow molecular weight standards in THF at 40°C.

The dynamic light scattering measurements were performed using a Malvern ZetaSizer (Nano-ZS, Malvern Instruments, Worcestershire, UK). The instrument was equipped with a He-Ne laser operating at 633 nm and an avalanche photodiode detector. Samples were filtered through a 0.45 μm Millex Millipore PVDF membrane prior to measurements. Cumulant analysis was applied to obtain the hydrodynamic diameter and polydispersity index of the nanoparticles. Measurements were performed in triplicate at room temperature. The constrained regularized CONTIN method was used to obtain the particle size distribution. UV-vis absorption spectra were recorded with an Agilent 8452A photodiode array spectrometer. Steady-state fluorescence spectra were recorded using a Varian Cary Eclipse fluorescence spectrophotometer.

HPLC analysis of curcumin was performed on a Waters chromatography system equipped with Waters 1525 μ binary HPLC pump, Waters 717plus autosampler, Waters Symmetry C18 5 μm and 4.6 × 150 mm column, Waters 2487 dual λ absorbance detector, and an IBM computer equipped with the Breeze software. The assay

was carried out at 25°C using a 7:3 v/v mixture of acetonitrile-0.5% w/v citric acid solution adjusted to pH 3.0 by 50% w/v aqueous KOH solution. The flow rate was 1.2 mL/min. The injection volume was 20 μL and the run time was 9 min. Curcumin, monitored by its absorbance at 420 nm, had a retention time ~7.1 min. A calibration curve ($r^2 \geq 0.999$) of curcumin was prepared using standard solutions ranging in concentration from 10 to 50 μg/mL prepared immediately prior to the assay. To assay curcumin content of different mikroarm micelles, a given volume of aqueous micellar solution was diluted 10 times by acetonitrile to break the micelle structure. The solution was filtered through 0.2 μm Millex Millipore nylon filter and assayed by HPLC. Curcumin encapsulation efficiency and loading capacity were calculated from the following equations:

$$\text{Curcumin encapsulation efficiency (weight \%)} = \frac{\text{weight of curcumin in the micelles}}{\text{Total weight of curcumin used initially}} \times 100 \quad (1)$$

$$\text{Curcumin loading capacity (weight \%)} = \frac{\text{weight of curcumin in the micelles}}{\text{Total weight of micelles tested}} \times 100 \quad (2)$$

Critical association concentration (CAC) of A₂B mikroarm micelles

Given volumes of pyrene stock solution in acetone (180 μM) were added to a series of 4 mL vials and the acetone was allowed to evaporate

overnight in the dark. Specified volumes of the micellar solutions were added to the vials having pyrene to obtain a polymer concentration ranging from 0.025 to 200 $\mu\text{g/mL}$. Pyrene concentration was kept constant at 6 μM . The pyrene/micellar solutions were equilibrated overnight in the dark. Excitation spectra were recorded from 260 to 360 nm at $\lambda_{\text{em}}=390$ nm (excitation and emission bandpass, 5 nm, respectively). The ratios of the pyrene fluorescence intensities at $\lambda=338$ and 333 nm (I_{338}/I_{333}) were calculated and plotted versus polymer concentration. The critical association concentration (CAC) values were determined from the graphs as the intersections of two straight lines (the horizontal line with an almost constant value of the ratio I_{338}/I_{333} and the vertical line with a steady increase in the ratio value).

Drug release studies

In vitro release of curcumin from miktoarm micelles was studied by the dialysis bag method in phosphate-buffered saline (PBS pH 7.4) containing 1% (v/v) Tween[®] 80. Tween[®] 80 was added to maintain perfect sink conditions since curcumin has limited solubility in PBS. Curcumin/miktoarm micellar solutions in deionized water (2 mL, [curcumin]=0.05-0.10 mg/mL) were introduced in a dialysis tube (MWCO = 6-8 kDa) and were dialyzed against 20 mL of the release medium maintained at 37°C. At predetermined time intervals, the whole medium was removed and replaced by fresh medium to maintain sink conditions. Curcumin solution at 0.1 mg/mL in a solvent mixture of PEG400-water-dimethylacetamide (45:40:15 v/v) was used as a control [26]. Care was taken during the experiments to protect Curcumin against light. Asorbic acid (1 mg/mL) was added to the release medium to protect Curcumin against degradation [27]. The concentration of the drug in the release samples was determined by HPLC as described above. The cumulative percent of drug released was plotted as a function of dialysis time.

Cell cultures

The human malignant glioblastoma multiforme cell line (U251N) American Type Culture Collection, ATCC #HTB-17). The U251N cell line has been discontinued; however, the current commercially available equivalent is U373 MG (ATCC #HTB-17). The cells were grown and maintained in Dulbecco's modified Eagle's medium (DMEM; Gibco BRL, Carlsbad, CA, USA) containing high glucose (4.5 g/L), 1% penicillin-streptomycin, and supplemented with 10% fetal bovine serum (FBS; Gibco BRL, Carlsbad, CA, USA). Cells were incubated at 37°C in a humidified environment with 5% CO₂. During cell splitting, cells were detached using trypsin/EDTA, collected in 15-mL conical tubes and centrifuged at 1,200 rpm for 4 minutes at room temperature. The cell pellet was then re-suspended in DMEM supplemented with 10% FBS. A million cells were seeded in a 75 cm² lasks (SARSTEDT, Newton, NC, USA) Cells doubling time was 24 hours. Medium was replaced every 2 days.

3-D Tumor spheroids preparation

Agarose (0.2 g) was added to 10 mL of serum free DMEM (2% weight/volume) in a 50 mL glass beakers, sealed with aluminum foil. Contents were then autoclaved for 20 minutes at 120°C with a pressure of 2 bar (departmental autoclave cycle #1). After, beakers was transferred to a sterile work bench and pipetted into 96-well microtiter plates at 75 μL /well. Agarose was left to set. U251N glioblastoma cells were then seeded into each well at a density of 5,000 cells/well using 0.22 micron filtered serum containing media. Tumor spheroids were allowed to grow for 4 days in incubator. Media of spheroids were changed every 2 days by replacing 50% of the growth media with fresh media.

MTT assay

Succinate-dehydrogenase dependent MTT reduction (MTT assay) was used for the detection of cellular mitochondrial metabolic activity. MTT assay was also used as an indirect, estimative assay for cell viability. Cells were seeded (50,000 cells/well) in 24-well, flat bottomed tissue culture plates (SARSTEDT; catalog number: 83.1836). Cells were treated 24 hours after seeding for a total treatment time of total of 24 hours. After treatment, the MTT reagent was added to the cells and incubated for 1 hour at 37°C. DMSO was then used to lyse the cells and to dissolve the formazan salt. Absorbance (at 595 nm) was measured with a micro-plate reader (Asys UVM340).

Labeling of cell nuclei with Hoechst 33258 for cell viability assessment

Cell viability was confirmed by cell counting. After treatment, cells were fixed with paraformaldehyde (4%) for 10 minutes at room temperature and washed three times with phosphate buffered saline (PBS). Fixed cell nuclei were then labeled with 10 μM Hoechst 33258 for 10 minutes and again washed three times with PBS. Fluorescent micrographs of labeled nuclei were captured using the Operetta imaging system (Perkin Elmer, excitation 360-400 nm, emission 410-480 nm). Seventeen pictures per well were captured with Operetta. Nuclei quantification was analyzed using the Harmony software.

Propidium iodide labeling

Necrotic cell death in tumor spheroids was analyzed by measuring fluorescence from propidium iodide (PI) labeling. After treatment, 50% of growth media was removed from each well of spheroid. Spheroids were then labeled with 1.5 μM PI and incubated for 2 h at 37°C. After labeling, 50% of media was removed and replaced by fresh growth media. Fluorescent pictures of nuclei labeled with PI were taken using Leica CTR4400 microscope (excitation 535 nm, emission 617 nm). Fluorescence was quantified by Image J software.

Results and Discussion

Synthesis of A₂B miktoarm polymers

The synthesis of A₂B miktoarm star polymers was achieved by an adaptation of our previously published procedure, using a core with orthogonal functionalities (1), and Cu(I) catalyzed alkyne azide click reaction in sequence with ring opening polymerization (ROP), (Figure 1A) [22]. The azide terminated-PEG₇₅₀ was synthesized starting from commercially available PEG mono methyl ether [25]. The acetylene units on 1 were employed to perform two simultaneous click reactions with PEG₇₅₀-azide to obtain compound 2. The completion of the reaction was confirmed by ¹H NMR, which showed the disappearance of acetylene protons, and the appearance of PEG and triazole protons. Macroinitiator 2 was subsequently employed to perform a series of ring opening polymerization reactions with variable amounts of ϵ -caprolactone monomer to construct a library of A₂B miktoarm stars

Sr. No	Polymer	Mn ^a (g/mole)	PDI
3a	(PEG ₇₇₅) ₂ -PCL ₄₇₀₀	6540	1.57
3b	(PEG ₇₇₅) ₂ -PCL ₇₈₀₀	9632	1.28
3c	(PEG ₇₇₅) ₂ -PCL ₈₈₀₀	10,605	1.38
3d	(PEG ₇₇₅) ₂ -PCL _{10,300}	12,105	1.49
3e	(PEG ₇₇₅) ₂ -PCL _{12,600}	14,327	1.21
3f	(PEG ₇₇₅) ₂ -PCL _{14,200}	16,000	1.27

^a: Determined from GPC measurement

Table 1: GPC analysis of miktoarm polymers.

with PCL molecular weights ranging from approximately 4700 to 14,000 Da (Table 1).

Self-assembly and micellization of A₂B mikroarm polymers

In order to get insights into the self-assembly behavior and drug loading capacity, a series of A₂B mikroarm stars, was examined where PEG arms were of molecular weight 750 Da and the molecular weight of the PCL arm ranged from 4.7 to 14.2 kDa (Table 1). Figure 1B shows schematic illustration of the polymer self-assembly and drug loading, in an aqueous environment. The self-assembly behavior of these copolymers in deionized water was studied using pyrene as a fluorescent probe. This method is widely used in the determination of polymeric micelle critical association concentration (CAC) due to its ease of application, versatility and reliability [28,29]. Pyrene excitation spectrum shows a red shift when it passes from aqueous environment to the hydrophobic core of polymeric micelles [30]. Excitation spectra of aqueous polymer solutions containing 6 μM pyrene and different polymer concentrations were recorded from 260 to 360 nm at λ_{em} = 390 nm. Semilogarithmic plots of the I₃₃₈/I₃₃₃ ratios versus the concentration of different (PEG₇₅₀)₂-PCL mikroarm polymers are shown in Figure 2A. The I₃₃₈/I₃₃₃ ratio remained almost constant ~0.7 at low polymer

concentration, and increased sharply when the polymer concentration reached its CAC. The results show that the CAC decreased from 1.32 μg/mL (0.20 μM) to 0.35 μg/mL (0.02 μM) as the PCL arm length increased from 4.7 to 14.2 kDa (Table 2). This is consistent with other reports showing that self-assembly occurs at lower polymer concentrations with the increase in the molecular weight of the hydrophobic block [19,31].

The structure of the micelles with and without curcumin was studied by ¹H NMR spectroscopy (Figure 3). This technique takes advantage of the reduced mobility of the protons forming the micelle core, which results in disappearance or broadening of their peaks. In contrast, the protons of the corona forming block maintain their mobility and have better resolution. ¹H NMR spectra of curcumin, (PEG₇₅₀)₂-PCL₄₇₀₀, and their mixture in CDCl₃, together with the blank and curcumin-loaded micelles in D₂O are shown in Figure 3. Characteristic signals of curcumin and (PEG₇₅₀)₂-PCL₄₇₀₀ were observed when they were dissolved in CDCl₃ (Figure 3A,B). The same signals were observed for curcumin/(PEG₇₅₀)₂-PCL₄₇₀₀ physical mixture in CDCl₃ (Figure 3C). In contrast, the spectrum of (PEG₇₅₀)₂-PCL₄₇₀₀ micelles without incorporated curcumin, in D₂O, showed signals characteristic of PEG protons (δ 3.51 ppm), confirming that they are well hydrated and

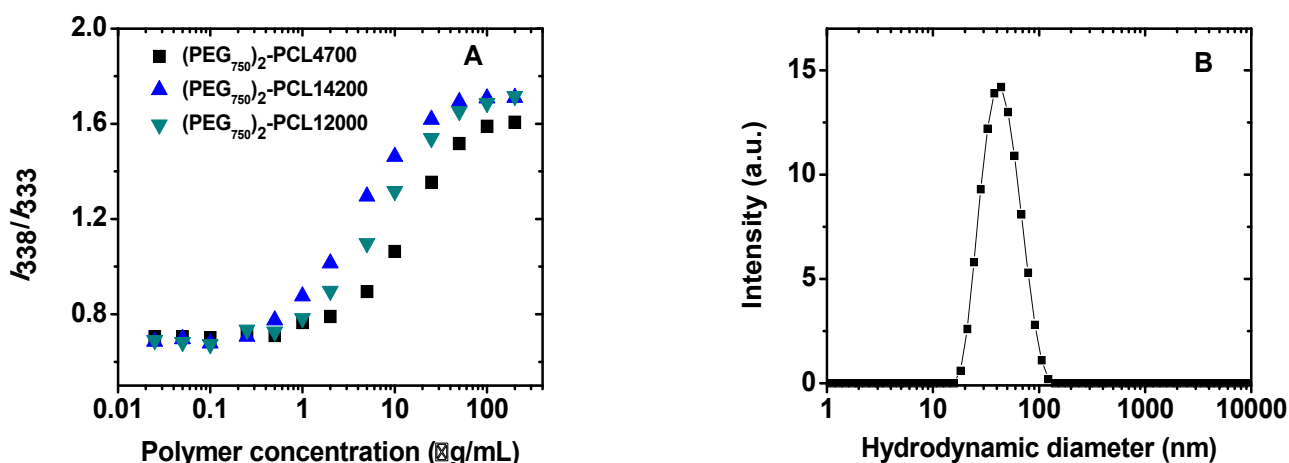


Figure 2: (A) Plots of intensity ratio (I_{338}/I_{333}) of pyrene excitation spectra ($\lambda_{em} = 390$ nm) vs concentration of different (PEG₇₅₀)₂-PCL mikroarm copolymers in water. (B) Distribution of the hydrodynamic diameter (D_H) of Curcumin/(PEG₇₅₀)₂-PCL₄₇₀₀ micelles (deionized water; polymer concentration, 0.5 g/L; θ , 90°, curcumin content ~ 8 wt.%).

Polymer	Micelle diameters		%DLb (wt.%)	%EEc (wt.%)	%DLd (mol%)	CACe (μg/ml)
	Blank micelles	curcumin micelles				
(PEG750) ₂ -PCL4700	47.3 ± 3.6	42.9 ± 0.5	6.0 ± 0.1	60.0 ± 0.8	50.5 ± 0.3	1.32
(PEG750) ₂ -PCL7800	45.9 ± 0.6	40.9 ± 0.6	4.6 ± 0.1	48.7 ± 1.4	55.3 ± 0.7	-
(PEG750) ₂ -PCL8800	63.3 ± 2.4	53.7 ± 1.6	4.6 ± 0.1	48.5 ± 0.6	57.7 ± 0.3	-
(PEG750) ₂ -PCL10300	57.8 ± 1.8	46.0 ± 1.3	5.3 ± 0.1	55.5 ± 0.6	64.1 ± 0.2	-
(PEG750) ₂ -PCL12000	55.3 ± 0.9	45.8 ± 1.0	5.2 ± 0.0	54.4 ± 0.2	66.7 ± 0.1	0.39
(PEG750) ₂ -PCL14200	46.6 ± 0.9	56.7 ± 2.9	6.5 ± 0.0	65.0 ± 0.3	73.5 ± 0.1	0.35

^aHydrodynamic diameter (nm), mean of three measurements ± SD

^bDrug loading (weight %)= $\frac{\text{weight of curcumin in the micelles}}{\text{weight of micelles tested}} \times 100$ mean of three measurements ± SD

^cEncapsulation efficiency (weight %)= $\frac{\text{weight of curcumin in the micelles}}{\text{Total weight of curcumin used initially}} \times 100$, mean of three measurements ± SD

^dDrug loaded (mol%) = $\frac{\text{molar concentration of curcumin in micelles}}{\text{molar concentration of micelles (curcumin+polymer)}} \times 100$, mean of three measurements ± SD

^eCritical association concentration in water

Table 2: Properties of A₂B mikroarm polymers based micelles with or without curcumin.

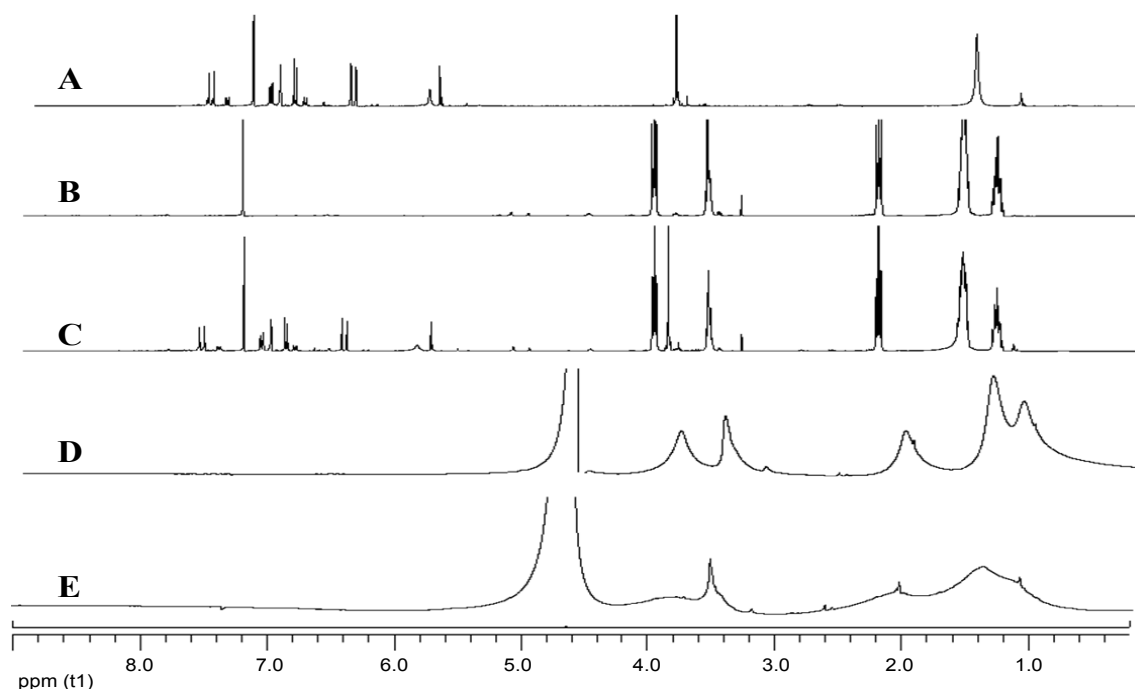


Figure 3: ¹H NMR spectra of curcumin in CDCl₃ (A), (PEG₇₅₀)₂-PCL₄₇₀₀ mikroarm in CDCl₃ (B), curcumin/(PEG₇₅₀)₂-PCL₄₇₀₀ mixture in CDCl₃ (C), blank (PEG₇₅₀)₂-PCL₄₇₀₀ mikroarm micelles in D₂O (D) and curcumin-loaded (PEG₇₅₀)₂-PCL₄₇₀₀ micelles in D₂O (E).

reserved their mobility (Figure 3D). The characteristic signals of the PCL arm protons appear weak and broad due to their incorporation into the micelles core and loss of mobility (Figure 3D). Similarly, the spectrum of curcumin/(PEG₇₅₀)₂-PCL₄₇₀₀ showed weak and broad curcumin and PCL signals and well-resolved PEG signals. Taken together, these results confirm the formation of core-corona structures in aqueous media (Figure 1B). Coating of nanoparticle surface with PEG chains usually results in prolonging nanoparticle circulation time *in vivo* [32].

The size and polydispersity index of the micelles prepared in water by the co-solvent evaporation method were studied by DLS [22]. Table 2 shows the hydrodynamic diameter (DH) for both curcumin-loaded and unloaded micelles of (PEG₇₅₀)₂-PCL miktoarms of different molecular weights. Considering the size of the blank micelles, there was a general trend of increase in the micelle hydrodynamic diameter with the increase in the molecular weight of the PCL arm. We confirmed by ¹H NMR studies that the PCL arm of the miktoarm polymers form the micelle core (Figure 3). This results in size increase with the increase in the hydrophobic segment molecular weight [18,33,34]. The incorporation of curcumin into the A₂B miktoarm micelles resulted in a slight decrease in their size for all the polymers (Table 2). Drug incorporation into the core of linear block copolymer micelles usually results in micelle size increase to accommodate the drug molecules [35,36]. However, there is no specific trend for the effect of drug loading on the size of star-shaped polymer micelles. In an earlier study, we had also observed that the incorporation of a hydrophobic drug, nimodipine into the micelles of A₂B star polymers did not change their size [18]. The incorporation of a hydrophobic drug into ABC miktoarm micelles can be accompanied both by an increase [22] or decrease in their size [37], suggesting that the change in micelle size depends on the specific drug/polymer combination. The polydispersity index was low (~0.2) for all the micelles with or without curcumin (Figure 2B).

To study the effect of PCL molecular weight on the drug loading capacity, a series of polymers was examined where PEG molecular weight was kept constant at 750 Da while the PCL molecular weight varied from 4700 to 14200 Da (Table 1). Curcumin was loaded into the micelles of these polymers at an initial drug/polymer weight ratio of 10 % and the actual loading capacity and encapsulation efficiency were calculated. Table 2 shows that the percent drug loading capacity varied from 4.5 to 6.5 weight % and was not affected by the PCL arm molecular weight. This was surprising since longer chain length of the hydrophobic arm was expected to increase the loading capacity of hydrophobic drugs [18]. Therefore, the actual loading capacity was calculated in terms of mole percent to get insights into the drug loading process. The results show that the mole percent of drug loading capacity increased from ~50 to 73 mole% when the PCL molecular weight increased from 4700 to 14200 Da. This is in agreement with other reports showing increase in drug loading with the increase in the hydrophobic polymer segment molecular weight [38,39].

Effect of curcumin/polymer weight feed ratio on micelle size and drug loading

Curcumin-loaded miktoarm polymer micelles were prepared at different curcumin/polymer weight ratios to obtain formulations with clinically relevant curcumin concentration while keeping polymer concentration at a minimum. Figure 4A shows the micelle hydrodynamic diameter and curcumin loading capacity as a function of curcumin/(PEG₇₅₀)₂-PCL₄₇₀₀ weight feed ratio and at a polymer concentration of 0.5 mg/mL. As the curcumin/polymer weight ratio increased from 0 to 20%, the micelle drug content increased from 0 to ~12 wt.%. The micelle curcumin content remained at this level (ca. 12%) with further increase in the curcumin/polymer ratio, indicating that the maximum drug loading was achieved at curcumin/polymer weight ratio of 20%. Under these conditions the drug encapsulation efficiency was calculated to be 60 wt. % and curcumin concentration in

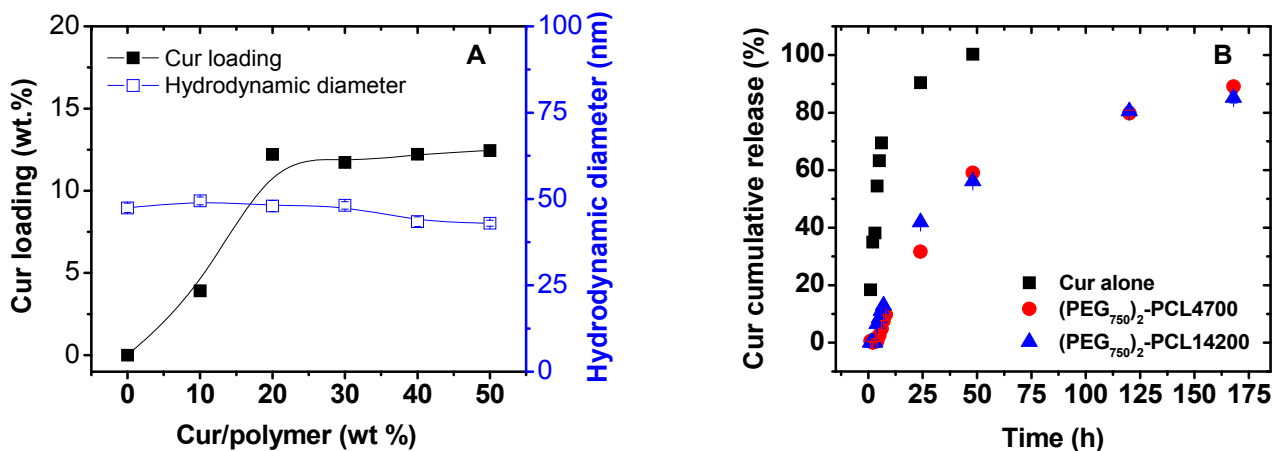


Figure 4: (A) Effect of drug/polymer weight feed ratio on drug loading capacity and micelle hydrodynamic diameter of curcumin/(PEG₇₅₀)₂-PCL₄₇₀₀ micelles prepared in deionized water at polymer concentration of 0.5 mg/mL. (B) Percent curcumin released from (PEG₇₅₀)₂-PCL₄₇₀₀ and (PEG₇₅₀)₂-PCL₁₄₂₀₀ micelles in PBS pH 7.4 having 1% (v/v) Tween® 80 at 37 °C.

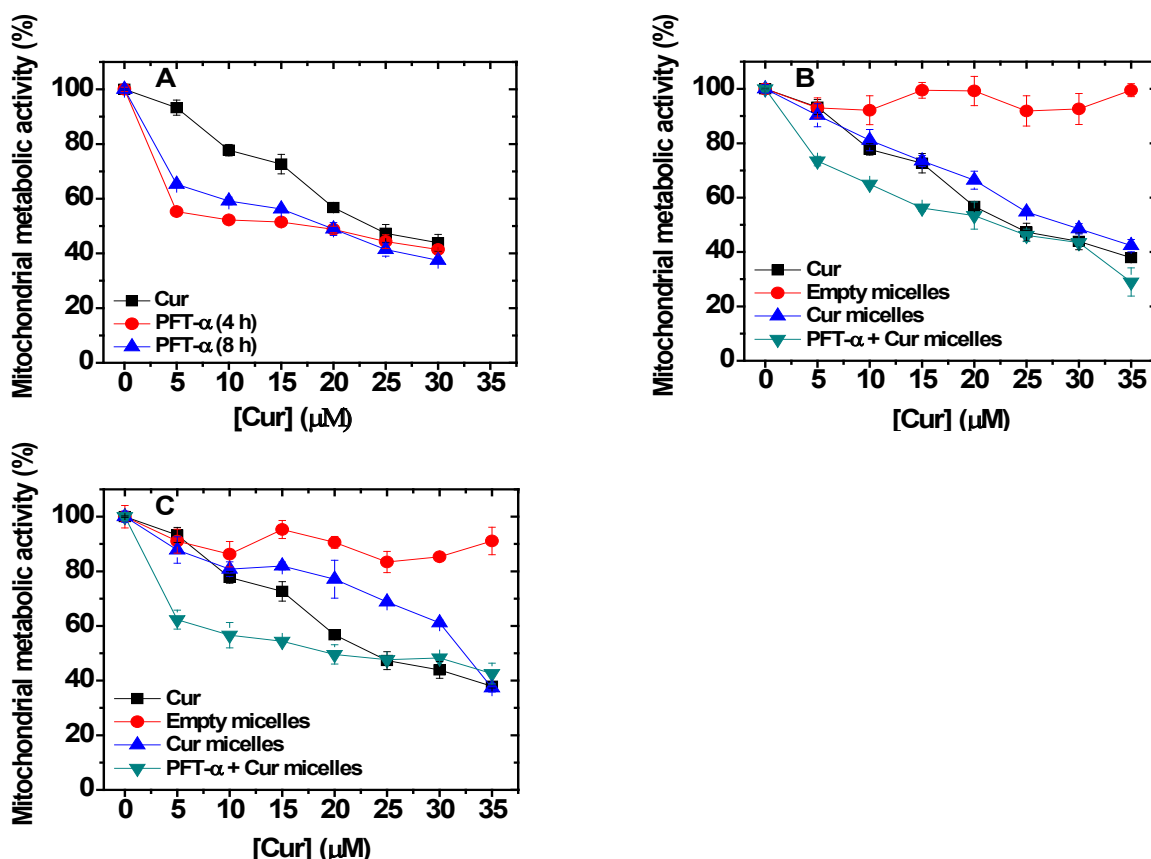


Figure 5: Curcumin alone and in micelles significantly decreased the mitochondrial metabolic activity of human glioblastoma cells. U251N human glioblastoma cells co-treated with pifithrin-α (PFT-α 50 μM) and curcumin alone ([curcumin]: 5-30 μM) or curcumin in micelles were assayed for changes in mitochondrial metabolic activity using the MTT assay. Cells were treated with: (A) increasing concentration of curcumin (5-30 μM) for 24, 20, 16 hours along with 0, 4, 8 hours of pifithrin-α, respectively, or pifithrin-α for 4 hours followed by a 20-hour treatment with curcumin incorporated into (PEG₇₅₀)₂-PCL₄₇₀₀ micelles ([curcumin]: 5-35 μM) (B) or curcumin incorporated into (PEG₇₅₀)₂-PCL₁₄₂₀₀ micelles ([curcumin]: 5-35 μM) (C). Treatments were significant (*p* < 0.05) vs untreated control starting at 10 μM (A), 10 μM (B), and 10 μM (C). Mean values ± SEM are calculated based on experiments ran in triplicates. Statistically significant differences from control were calculated using a *t*-test of OriginPro software.

water was ~60 µg/mL. By increasing polymer concentration from 0.5 to 2.0 mg/mL, curcumin concentration in water increased from ~60 to ~390 µg/mL. Knowing that curcumin aqueous solubility is 11 ng/mL, this represents more than 35,000 times enhancement in its aqueous solubility [13]. The effect of the curcumin/(PEG₇₅₀)₂-PCL₄₇₀₀ feed weight ratio on the micelle size did not show the same trend as that on the drug loading capacity (Figure 4A). Thus, the micelle hydrodynamic diameter remained almost constant till curcumin/polymer ratio of 30%, after which it slightly decreased.

In vitro curcumin release from A₂B miktoarm micelles

The dialysis bag method was used to evaluate the *in vitro* release behavior of curcumin from miktoarm micelles. The release medium was PBS pH 7.4 containing 1% (v/v) Tween® 80 which is a low molecular weight non-ionic surfactant that can be added to release media to maintain sink conditions for hydrophobic drugs [40,41]. Curcumin solubility in the release medium was 240.8 µg/mL confirming the maintenance of sink conditions during the release experiment given the release volume (20 mL) and curcumin amounts in the micelles (100-200 µg). Curcumin alone, used as a control rapidly diffused through

the dialysis membrane and almost complete release was observed after 24 h (Figure 4B). In contrast, curcumin incorporated into (PEG₇₅₀)₂-PCL₄₇₀₀ and (PEG₇₅₀)₂-PCL₁₄₂₀₀ micelles was released at a much slower rate. Around 85% of curcumin content in the micelles was released after 7 days of dialysis time. Curcumin release pattern was not affected by the molecular weight of the PCL arm. This finding is consistent with previously published results [18]. These results confirm the ability of these miktoarm micelles to sustain the release of curcumin, which may result in reduced frequency of drug administration and better patient compliance.

Inhibition of glioblastoma cell growth by curcumin in A₂B micelles and in combination with other drugs

We first established concentration- and time-dependent changes in glioblastoma U251N by measuring mitochondrial metabolic activity and viability following the treatment with curcumin, both free and incorporated into micelles (Figures 5 and 6). Although there was a concentration-dependent decline in mitochondrial activity, curcumin alone (0.1-35 µM) or incorporated in the A₂B micelles (maximal concentration 17.5 µM) did not adequately abolish glioblastoma cell

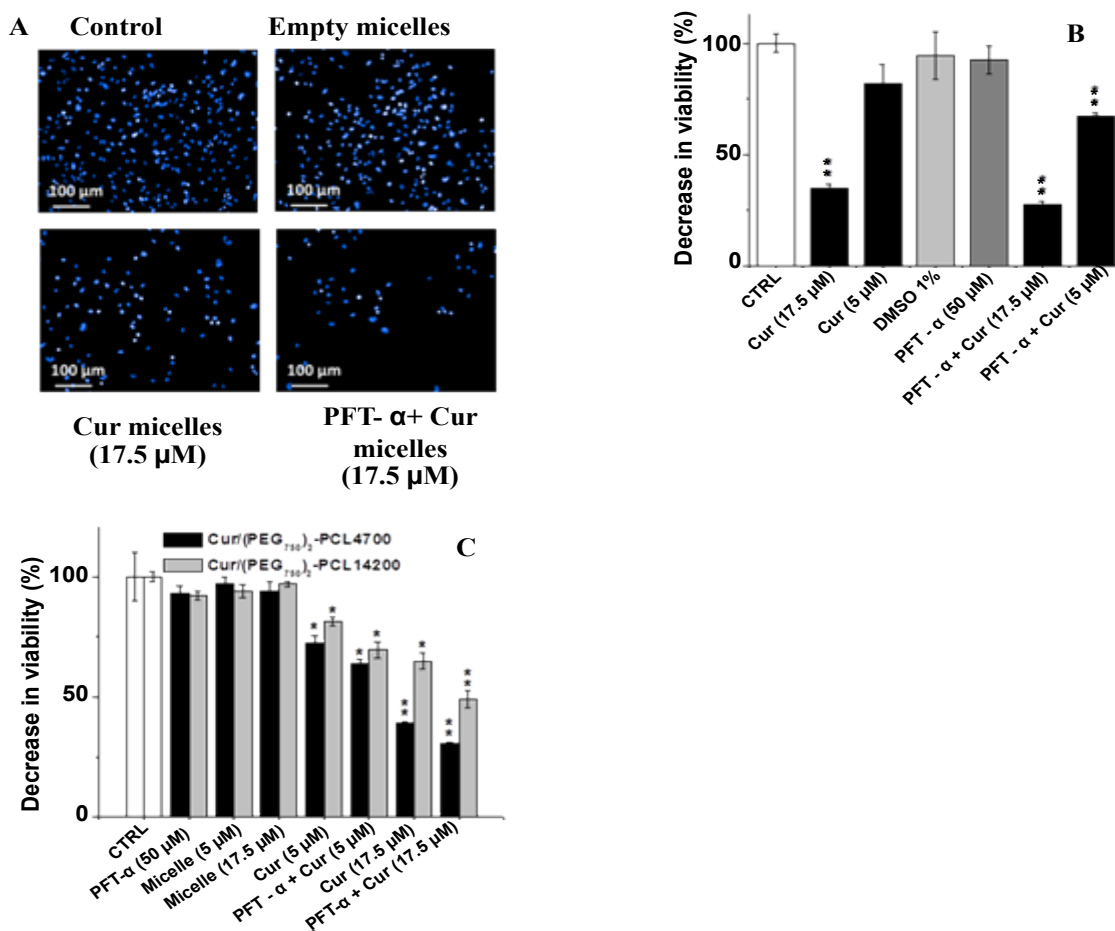


Figure 6: Curcumin alone and incorporated in micelles significantly increased human glioblastoma cell death. U251N cells were treated with curcumin alone (curcumin) or curcumin incorporated in micelles (curcumin micelles, (PEG₇₅₀)₂-PCL₄₇₀₀) for 24 or 20 hours with 0 or 4 hours of pifithrin-α (50 µM), for a total of 24 hours. Cells were then fixed and stained with the fluorescent Hoechst dye (10 µM, blue). Images were taken directly from the plate using Operetta imaging system (Perkin Elmer) and cell number was analyzed using the Harmony software. Viability of cells treated with curcumin alone (B) or curcumin in micelles (C) ((PEG₇₅₀)₂-PCL₄₇₀₀ or (PEG₇₅₀)₂-PCL₁₄₂₀₀) is expressed relative to untreated cells. Mean values ± SEM are calculated based on experiments ran in triplicates. Statistically significant differences from untreated control were calculated using a *t*-test of OriginPro software and indicated by * (*p* < 0.05) and ** (*p* < 0.01).

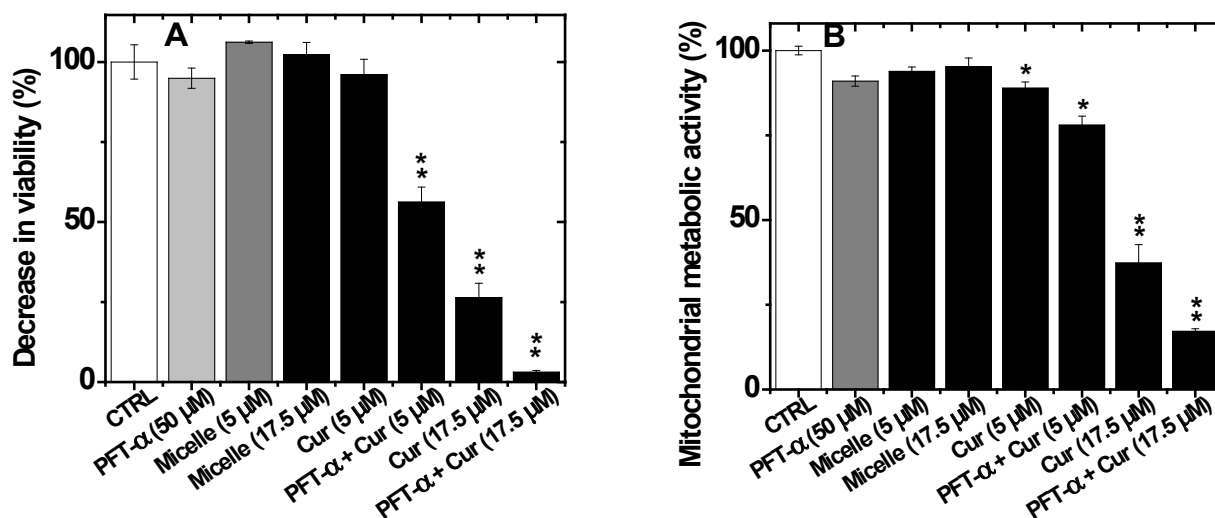


Figure 7: 96-hour treatment with curcumin incorporated in micelles alone and with co-treatments significantly increased human glioblastoma cell death. Cells were then fixed and stained after treatment with the fluorescent Hoechst dye (10 μM, blue). Images were taken directly from the plate using Operetta imaging system (Perkin Elmer) and cell number was analyzed using the Harmony software. (A) U251N human glioblastoma cells co-treated with pifithrin-α (PFT-α 50 μM, 4 hours) and curcumin in micelles (Cur, 92 hours) ((PEG750)2-PCL4700) or curcumin in micelles alone (96 hours). Cell viability was analyzed by quantification of Hoechst stained nuclei. (B) U251N human glioblastoma cells co-treated with pifithrin-α (PFT-α 50 μM) and curcumin in micelles (Cur) ((PEG750)2-PCL4700) or curcumin in micelles alone were assayed for changes in mitochondrial metabolic activity using the MTT assay. Cells were treated with: 2 different concentration of curcumin in micelles (5 or 17.5 μM) for 96, 92 hours along with 0, 4 hours of pifithrin-α, respectively, for a total treatment time of 96 hours. (n=2). Statistically significant differences from untreated control were calculated using a t-test of OriginPro software and indicated by * (p < 0.05) and ** (p < 0.01).

growth after 24 hours. To enhance curcumin cell killing effect an inhibitor of p53, pifitrin (50 μM) was used as a putative sensitizer to enhance cell death. Although pifitrin increased glioblastoma cell death when combined with curcumin by about 13%, there were still 40- 60% metabolically active cells (Figure 5A). Such an intervention would not be acceptable in clinics because of the re-occurrence of tumor growth and possibly greater glioblastoma resistance to further therapeutic interventions. The poor outcome was even more striking in glioblastoma spheroids (3D cultures), a model which is more appropriate than cell monolayers. Spheroids represent an intermediate between the monolayers and xenografts and they are increasingly used for screening of anticancer agents [42-45]. The effectiveness of two types of A₂B micelles was marginally different suggesting that shorter polycaprolactone chains (PCL 4700) did not significantly increase the rate of curcumin release in the intracellular and extracellular biological environment (cf. micelles with PCL 14200). Surprisingly, these differences in PCL chain lengths contributed to different drug loading capacity (Table 2). PCL size did not seem to play a role in curcumin effectiveness in spheroid cultures.

Since mitochondrial metabolic activity does not necessarily provide the quantitative data for cell viability, we performed cell counting (Figure 6). These experiments were done by labeling the cells with the fluorescent dye Hoechst 33342 and propidium iodide. Results from the cell counting experiments corroborated the data from mitochondrial metabolic activity (Figure 5). Glioblastoma cells were treated for prolonged time period (96 hours) and the results clearly showed that long-term treatments are indeed required to completely abolish GBM cell survival (Figure 7). Moreover, the data indicated that repeated exposure to the drugs with or without sensitization with pifitrin and temozolomide. Temozolomide is commonly used as a drug of choice in glioblastoma [46].

Temozolomide exerts its anticancer effect by methylating nuclear

DNA thereby damaging nuclear structure and function leading to the cell cycle arrest [47]. Several formulations for temozolomide were developed (e.g. poly(lactide-coglycolide (PLGA) microspheres and magnetic nanoparticles [48,49]. We used this agent as standard to compare the effectiveness of curcumin alone and in combination with pifitrin.

Conclusion

Combination therapy using nanocarriers that could enhance the efficacy of hydrophobic drugs which are poorly soluble in an aqueous medium constitute a topical area of research. Amphiphilic miktoarm polymers have offered an exciting platform to address this issue, and we have demonstrated that A₂B type miktoarm stars constructed using alkyne-azide click and ring opening polymerization reactions, self-assemble into spherical micelles and help enhance aqueous solubility and sustained release of curcumin. The combination of curcumin loaded micelles with pifitrin and temozolomide were highly effective in causing glioblastoma cell death. Collectively, our studies suggest that A₂B miktoarm star based polymers offer opportunities to construct nanocarriers for combination therapy involving unstable and poorly water soluble drugs such as curcumin which is of particular interest for the *in vivo* investigations.

Acknowledgement

We would like to thank Natural Sciences and Engineering Research Council of Canada, (NSERC), Canadian Institutes of Health Research (CIHR) and Fonds de Recherche en Santé du Québec (FRSQ) and Centre for Self-Assembled Chemical Structures (FQRNT, Quebec, Canada) for financial support.

References

- Inda MD, Bonavia R, Seoane J (2014) Glioblastoma multiforme: a look inside its heterogeneous nature. *Cancers (Basel)* 6: 226-239.
- Omuro A, DeAngelis LM (2013) Glioblastoma and other malignant gliomas: a clinical review. *JAMA* 310: 1842-1850.

3. Yung WK, Albright RE, Olson J, Fredericks R, Fink K, et al. (2000) A phase II study of temozolomide vs. procarbazine in patients with glioblastoma multiforme at first relapse. *Br J Cancer* 83: 588-593.
4. Brem H, Piantadosi S, Burger PC, Walker M, Selker R, et al. (1995) Placebo-controlled trial of safety and efficacy of intraoperative controlled delivery by biodegradable polymers of chemotherapy for recurrent gliomas. The Polymer-brain Tumor Treatment Group. *Lancet* 345: 1008-1012.
5. Morshed RA, Cheng Y, Auffinger B, Wegscheid ML, Lesniak MS (2013) The potential of polymeric micelles in the context of glioblastoma therapy. *Front Pharmacol* 4: 157.
6. Yi N, Oh B, Kim HA, Lee M (2014) Combined delivery of BCNU and VEGF siRNA using amphiphilic peptides for glioblastoma. *J Drug Target* 22: 156-164.
7. Miura Y, Takenaka T, Toh K, Wu S, Nishihara H, et al. (2013) Cyclic RGD-linked polymeric micelles for targeted delivery of platinum anticancer drugs to glioblastoma through the blood-brain tumor barrier. *ACS Nano* 7: 8583-8592.
8. Goel A, Kunnumakkara AB, Aggarwal BB (2008) Curcumin as "Curecumin": from kitchen to clinic. *Biochem Pharmacol* 75: 787-809.
9. Sun M, Su X, Ding B, He X, Liu X, et al. (2012) Advances in nanotechnology-based delivery systems for curcumin. *Nanomedicine (Lond)* 7: 1085-1100.
10. Maheshwari RK, Singh AK, Gaddipati J, Srimal RC (2006) Multiple biological activities of curcumin: a short review. *Life Sci* 78: 2081-2087.
11. Anand P, Sundaram C, Jhurani S, Kunnumakkara AB, Aggarwal BB (2008) Curcumin and cancer: an "old-age" disease with an "age-old" solution. *Cancer Lett* 267: 133-164.
12. Anand P, Kunnumakkara AB, Newman RA, Aggarwal BB (2007) Bioavailability of curcumin: problems and promises. *Mol Pharm* 4: 807-818.
13. Tønnesen HH, Måsson M, Loftsson T (2002) Studies of curcumin and curcuminoids. XXVII. Cyclodextrin complexation: solubility, chemical and photochemical stability. *Int J Pharm* 244: 127-135.
14. Wang YJ, Pan MH, Cheng AL, Lin LI, Ho YS, et al. (1997) Stability of curcumin in buffer solutions and characterization of its degradation products. *J Pharm Biomed Anal* 15: 1867-1876.
15. Khanna K, Varshney S, Kakkar A (2010) Miktoarm star polymers: advances in synthesis, self-assembly, and applications. *Polym Chem* 1: 1171-1185.
16. Elzubair A, Elias CN, Suarez JC, Lopes HP, Vieira MV (2006) The physical characterization of a thermoplastic polymer for endodontic obturation. *J Dent* 34: 784-789.
17. Soliman GM, Sharma A, Maysinger D, Kakkar A (2011) Dendrimers and miktoarm polymers based multivalent nanocarriers for efficient and targeted drug delivery. *Chem Commun (Camb)* 47: 9572-9587.
18. Soliman GM, Sharma R, Choi AO, Varshney SK, Winnik FM, et al. (2010) Tailoring the efficacy of nimodipine drug delivery using nanocarriers based on A2B miktoarm star polymers. *Biomaterials* 31: 8382-8392.
19. Yin H, Kang HC, Huh KM, Bae YH (2012) Biocompatible, pH-sensitive AB2 miktoarm polymer-based polymersomes: preparation, characterization, and acidic pH-activated nanostructural transformation. *J Mater Chem* 22: 19168-19178.
20. Kulthe SS, Choudhari YM, Inamdar NN, Mourya V (2012) Polymeric micelles: authoritative aspects for drug delivery. *Des Monomers Polym* 15: 465-521.
21. Owen SC, Chan DPY, Shoichet MS (2012) Polymeric micelle stability. *Nano Today* 7: 53-65.
22. Sharma A, Soliman GM, A-Hajaj N, Sharma R, Maysinger D, et al. (2012) Design and evaluation of multifunctional nanocarriers for selective delivery of coenzyme Q10 to mitochondria. *Biomacromolecules* 13: 239-252.
23. Svenson S (2013) Theranostics: are we there yet? *Mol Pharm* 10: 848-856.
24. Liu J, Chen S, Lv L, Song L, Guo S, et al. (2013) Recent progress in studying curcumin and its nano-preparations for cancer therapy. *Curr Pharm Des* 19: 1974-1993.
25. Gao H, Matyjaszewski K (2007) Synthesis of molecular brushes by "grafting onto" method: combination of ATRP and click reactions. *J Am Chem Soc* 129: 6633-6639.
26. Song Z, Feng R, Sun M, Guo C, Gao Y, et al. (2011) Curcumin-loaded PLGA-PEG-PLGA triblock copolymeric micelles: Preparation, pharmacokinetics and distribution in vivo. *J Colloid Interface Sci* 354: 116-123.
27. Oetari S, Sudibyo M, Commandeur JN, Samhoedi R, Vermeulen NP (1996) Effects of curcumin on cytochrome P450 and glutathione S-transferase activities in rat liver. *Biochem Pharmacol* 51: 39-45.
28. Riess G (2003) Micellization of block copolymers. *Prog Polym Sci* 28: 1107-1170.
29. Huang X, Jiang X, Yang Q, Chu Y, Zhang G, et al. (2013) Triple-stimuli (pH/thermo/reduction) sensitive copolymers for intracellular drug delivery. *J Mater Chem B* 1: 1860-1868.
30. Lee K, Shin SC, Oh I (2003) Fluorescence spectroscopy studies on micellization of poloxamer 407 solution. *Arch Pharm Res* 26: 653-658.
31. Bury K, Du Prez F, Neugebauer D (2013) Self-assembling linear and star shaped poly(μ -caprolactone)/poly((meth)acrylic acid) block copolymers as carriers of indomethacin and quercetin. *Macromol Biosci* 13: 1520-1530.
32. Dufort S, Sancey L, Coll JL (2012) Physico-chemical parameters that govern nanoparticles fate also dictate rules for their molecular evolution. *Adv Drug Deliv Rev* 64: 179-189.
33. Gou PF, Zhu WP, Shen ZQ (2010) Synthesis, self-assembly, and drug-loading capacity of well-defined cyclodextrin-centered drug-conjugated amphiphilic A(14)B(7) Miktoarm star copolymers based on poly(epsilon-caprolactone) and poly(ethylene glycol). *Biomacromolecules* 11: 934-943.
34. Stolnik S, Heald CR, Neal J, Garnett MC, Davis SS, et al. (2001) Polylactide-poly(ethylene glycol) micellar-like particles as potential drug carriers: production, colloidal properties and biological performance. *J Drug Target* 9: 361-378.
35. Liu L, Li CX, Li XC, Yuan Z, An YL, et al. (2001) Biodegradable polylactide/poly(ethylene glycol)/polylactide triblock copolymer micelles as anticancer drug carriers. *J Appl Polym Sci* 80: 1976-1982.
36. Huh KM, Lee SC, Cho YW, Lee J, Jeong JH, et al. (2005) Hydrotropic polymer micelle system for delivery of paclitaxel. *J Control Release* 101: 59-68.
37. Pu Y, Zhang L, Zheng H, He B, Gu Z (2014) Synthesis and drug release of star-shaped poly(benzyl L-aspartate)-block-poly(ethylene glycol) copolymers with POSS cores. *Macromol Biosci* 14: 289-297.
38. Lim Soo P, Lovric J, Davidson P, Maysinger D, Eisenberg A (2005) Polycaprolactone-block-poly(ethylene oxide) micelles: a nanodelivery system for 17beta-estradiol. *Mol Pharm* 2: 519-527.
39. Shuai X, Ai H, Nasongkla N, Kim S, Gao J (2004) Micellar carriers based on block copolymers of poly(epsilon-caprolactone) and poly(ethylene glycol) for doxorubicin delivery. *J Control Release* 98: 415-426.
40. Gong C, Wu Q, Wang Y, Zhang D, Luo F, et al. (2013) A biodegradable hydrogel system containing curcumin encapsulated in micelles for cutaneous wound healing. *Biomaterials* 34: 6377-6387.
41. Wang F, Zhang D, Zhang Q, Chen Y, Zheng D, et al. (2011) Synergistic effect of folate-mediated targeting and verapamil-mediated P-gp inhibition with paclitaxel-polymer micelles to overcome multi-drug resistance. *Biomaterials* 32: 9444-9456.
42. Cheng AL, Hsu CH, Lin JK, Hsu MM, Ho YF, et al. (2001) Phase I clinical trial of curcumin, a chemopreventive agent, in patients with high-risk or pre-malignant lesions. *Anticancer Res* 21: 2895-2900.
43. Diinawaz F, Sahoo SK (2013) Enhanced accumulation of curcumin and temozolomide loaded magnetic nanoparticles executes profound cytotoxic effect in glioblastoma spheroid model. *Eur J Pharm Biopharm* 85: 452-462.
44. Matokanovic M, Barisic K, Filipovic-Grcic J, Maysinger D (2013) Hsp70 silencing with siRNA in nanocarriers enhances cancer cell death induced by the inhibitor of Hsp90. *Eur J Pharm Sci* 50: 149-158.
45. Breslin S, O'Driscoll L (2013) Three-dimensional cell culture: the missing link in drug discovery. *Drug Discov Today* 18: 240-249.
46. Hart MG, Garside R, Rogers G, Stein K, Grant R (2013) Temozolomide for high grade glioma. *Cochrane Database Syst Rev*.
47. Shen W, Hu JA, Zheng JS (2014) Mechanism of temozolomide-induced antitumour effects on glioma cells. *J Int Med Res* 42: 164-172.
48. Ling Y, Wei K, Zou F, Zhong S (2012) Temozolomide loaded PLGA-based superparamagnetic nanoparticles for magnetic resonance imaging and treatment of malignant glioma. *Int J Pharm* 430: 266-275.
49. Zhang D, Tian A, Xue X, Wang M, Qiu B, et al. (2012) The Effect of Temozolomide/Poly(lactide-co-glycolide) (PLGA)/Nano-Hydroxyapatite Microspheres on Glioma U87 Cells Behavior. *Int J Mol Sci* 13: 1109-1125.